Bone Reports 14 (2021) 101096

Contents lists available at ScienceDirect

Bone Reports

journal homepage: www.elsevier.com/locate/bonr

Plant-derived soybean peroxidase stimulates osteoblast collagen biosynthesis, matrix mineralization, and accelerates bone regeneration in a sheep model

Alexandra J. Barker [b], Agnes Arthur [d,e], Mark O. DeNichilo [f], Romana Panagopoulos [c], Stan Gronthos [d,e], Peter J. Anderson [d,f,g,i], Andrew C.W. Zannettino [a,e,h,i], Andreas Evdokiou [c,1], Vasilios Panagopoulos [a,c,e,*,1]

[a] Myeloma Research Laboratory, Adelaide Medical School, Faculty of Health and Medical Sciences, University of Adelaide, Adelaide, Australia
[b] Musculoskeletal Biology Research Laboratory, Clinical and Health Sciences, University of South Australia, Adelaide, Australia
[c] Breast Cancer Research Unit, School of Medicine, Discipline of Surgery and Orthopaedics, Basil Hetzel Institute, University of Adelaide, Adelaide, Australia
[d] Mesenchymal Stem Cell Laboratory, Adelaide Medical School, Faculty of Health and Medical Sciences, University of Adelaide, Adelaide, Australia
[e] Precision Medicine Theme, South Australian Health and Medical Research Institute, Adelaide, Australia
[f] Centre for Cancer Biology, University of South Australia, Adelaide, Australia
[g] Australian Craniofacial Unit, Women's and Children's Hospital, Department of Paediatrics and Dentistry, University of Adelaide, Adelaide, Australia
[h] Department of Haematology, Royal Adelaide Hospital, Adelaide, Australia
[i] Central Adelaide Local Health Network, Adelaide, Australia

ARTICLE INFO

Keywords:
Soybean peroxidase
Collagen biosynthesis
Matrix mineralization
Bone repair
Osteoinductive agent
Osteoblast

ABSTRACT

Bone defects arising from fractures or disease represent a significant problem for surgeons to manage and are a substantial economic burden on the healthcare economy. Recent advances in the development of biomaterial substitutes provides an attractive alternative to the current "gold standard" autologous bone grafting. Despite ongoing research, we are yet to identify cost effective biocompatible, osteo-inductive factors that stimulate controlled, accelerated bone regeneration.We have recently reported that enzymes with peroxidase activity possess previously unrecognised roles in extracellular matrix biosynthesis, angiogenesis and osteoclastogenesis, which are essential processes in bone remodelling and repair. Here, we report for the first time, that plant-derived soybean peroxidase (SBP) possesses pro-osteogenic ability by promoting collagen I biosynthesis and matrix mineralization of human osteoblasts *in vitro*. Mechanistically, SBP regulates osteogenic genes responsible for inflammation, extracellular matrix remodelling and ossification, which are necessary for normal bone healing. Furthermore, SBP was shown to have osteo-inductive properties, that when combined with commercially available biphasic calcium phosphate (BCP) granules can accelerate bone repair in a critical size long bone defect ovine model. Micro-CT analysis showed that SBP when combined with commercially available biphasic calcium phosphate (BCP) granules significantly increased bone formation within the defects as early as 4 weeks compared to BCP alone. Histomorphometric assessment demonstrated accelerated bone formation prominent at the defect margins and surrounding individual BCP granules, with evidence of intramembranous ossification. These results highlight the capacity of SBP to be an effective regulator of osteoblastic function and may be beneficial as a new and cost effective osteo-inductive agent to accelerate repair of large bone defects.

1. Introduction

Large bone defects which occur as a result of trauma, tumor resection and fractures remain a significant problem in regenerative medicine. Autogenous bone graft transplantation is the current "gold standard" for the treatment of large bone defects due to their osteogenicity, osteoconductivity and osteoinductivity potential (Jimi et al., 2012; Helm et al., 2001). However, the amount of autologous bone which can be

* Corresponding author at: Myeloma Research Laboratory, Level 5 South, South Australian Health and Medical Research Institute, Adelaide SA 500, Australia.
E-mail address: bill.panagopoulos@adelaide.edu.au (V. Panagopoulos).
[1] These authors contributed equally to the work.

https://doi.org/10.1016/j.bonr.2021.101096
Received 2 December 2020; Received in revised form 29 April 2021; Accepted 21 May 2021
Available online 27 May 2021

harvested is limited and is associated with the potential for donor site morbidity at the second surgical site, resulting in higher complication rates and longer rehabilitation times (Almaiman et al., 2013; Finkemeier, 2002; Gamradt and Lieberman, 2003; Homma et al., 2013). To address these limitations, biological alternatives such as allografts and xenografts have been developed, however these are suboptimal due to limited availability, high cost, immunogenicity and poor osteoinductivity (Betz, 2002).

The use of synthetic bone graft substitutes, often in the form of calcium phosphate ceramics is increasing, owing to their ability to eliminate many of the issues associated with the use of autologous and autograft bone (Fillingham and Jacobs, 2016). Of these, synthetic materials comprised of β-tricalcium phosphate (β-TCP) and hydroxyapatite (HA), termed biphasic calcium phosphate (BCP) have been studied extensively (Bouler et al., 2017), as the composition of these minerals are comparable to normal bone tissue (Kivrak and Taş, 1998). Although these materials demonstrate high biocompatibility and osteoconductive properties (Gronthos et al., 2000; Wongwitwichot et al., 2010), new bone formation is often limited due to poor osteoinductive capabilities (Yuan et al., 2002). This limitation can be overcome with the incorporation of osteoinductive agents such as BMP-2 to accelerate osteogenesis (Szpalski et al., 2012). BMP-2 is currently the only approved osteoinductive factor used as a bone graft substitute. However, with increasing clinical use a number of drawbacks to BMP-2 have emerged, including ectopic bone formation, osteoclast mediated bone resorption (Tannoury and An, 2014; James et al., 2016) and high dosage levels, raising concerns about efficacy and cost effectiveness (Yaszemski et al., 1996). Therefore, there is an urgent need to identify new biological agents with osteoinductive capabilities that accelerate bone formation and remodelling without adverse effects.

Peroxidases are a group of haem-containing enzymes found in animals, plants and micro-organisms (Hiraga et al., 2001). This family of enzymes share the same catalytic mechanism, and convert hydrogen peroxide and halide ions into hypohalous acid, which is one of the most reactive oxidants produced *in vivo* and is responsible for peroxidase antimicrobial actions (Aruoma and Halliwell, 1987). We have recently discovered new functional roles for peroxidase enzymes, including mammalian myeloperoxidase (MPO) and eosinophil peroxidase (EPO), plant-derived soybean peroxidase (SBP) and horseradish peroxidase (HRP). These roles include the ability to regulate fibroblast collagen extracellular matrix (ECM) biosynthesis (DeNichilo et al., 2015), drive angiogenesis (Panagopoulos et al., 2015) and inhibit osteoclastogenesis (Panagopoulos et al., 2017a). Collectively, these findings suggest that peroxidases may have an important role in tissue repair. In addition, we have recently reported new roles for mammalian peroxidases in bone repair, by their ability to promote osteoblast collagen biosynthesis, osteogenic gene expression and bone matrix mineralization (DeNichilo et al., 2016). SBP is highly biologically active and exceedingly stable at high temperatures and low pH (Henriksen et al., 2001). SBP is an attractive candidate to investigate in the context of bone repair due to low economical production costs and previous anectodal studies that have suggested consumption of soy products can elicit favourable effects on bone health and mineral density (Zhang et al., 2005; Shams-White et al., 2018).

Herein, we report for the first time, that SBP has the ability to stimulate the release of collagen type I and promote matrix mineralization by primary human osteoblasts. We also evaluated the osteoinductive capacity of SBP, in combination with a commercially available BCP, to accelerate bone regeneration in critical size defects created in the long bones of sheep.

2. Materials and methods

2.1. Ethics statement

Normal human bone tissue was obtained with informed written donor consent, and approved for use by the human ethics committee of the Royal Adelaide Hospital/University of Adelaide (Approval No. RAH 090101). The use of sheep was approved by the Animal Ethics Committee of the University of Adelaide (M-2015-044A) and conducted at the Medical Engineering Research Facility, Chermside, QLD.

2.2. Animals

Four male castrated, wethers sheep aged 3–5 years, weighing 56–69 kg (mean: 60; SD ± 5.9) were randomly assigned with even distribution, to receive the experimental treatment in either the left or right hind limb to eliminate bias. The opposing hind limb received the control treatment.

2.3. Osteoblast cell culture

Normal human bone-derived osteoblasts were isolated from intertrochanteric trabecular bone samples from three donors of both genders (1 male and 2 female), aged between 46 and 67 years, undergoing primary hip and knee replacement surgery, as described previously (Atkins et al., 2003). Human osteoblasts were culture expanded using Dulbecco's Modified Eagle's Medium (DMEM; high glucose with no ascorbic acid; AA), supplemented with 2 mmol/L glutamine, 100 IU/mL penicillin, 100 μg/mL streptomycin, 20 mmol/L HEPES, and 10% foetal bovine serum (FBS; Invitrogen Life Technologies, Carlsbad, CA) in a 5% CO_2-containing humidified atmosphere. These cells maintain an osteoblastic phenotype in culture and stained positive for alkaline phosphatase activity (DeNichilo et al., 2016).

2.4. Collagen I enzyme-linked immunosorbent assay (ELISA)

To evaluate the effect of SBP on collagen I production, osteoblasts were cultured and treated as previously described (DeNichilo et al., 2016). Briefly, osteoblasts were cultured in 96-well plates for 5 days in complete growth media until confluent. Cells were starved overnight in serum-free DMEM and then stimulated for an additional 72 h in serum-free DMEM containing either AA 2-phosphate at 100 μmol/L (Wako Chemical Industries, Osaka, Japan) as a positive control, or with increasing concentrations of SBP (Bio-Research Products, North Liberty, IA) in the absence of AA supplementation. Osteoblast basal-conditioned media was then collected for measurement of secreted, soluble type I collagen by ELISA. Cell viability was then assessed using the alamarBlue™ fluorescent dye assay (Invitrogen Life Technologies), according to manufacturer's instructions. Fluorescence was measured at wavelengths of 530 nm excitation and 595 nm emission using a FLUOstar Optima plate reader (BMG Labtek Australia, Mornington, VIC).

The quantity of soluble type I collagen in cell-conditioned medium was measured by a direct coat enzyme-linked immunosorbent assay method, as previously described (DeNichilo et al., 2016). Samples and standards were added to a 96-well Maxisorp plate (Nunc) and left at 4 °C overnight. The plate was then washed with phosphate-buffered saline (PBS) with 0.05% Tween, 2.5% bovine serum albumin (BSA)/PBS blocking solution added to each well and the plate incubated for 1 h at room temperature. The plate was then washed and primary antibody (0.25 μg/mL rabbit anti-human-collagen I polyclonal; Rockland Immunochemicals, Limerick, PA) in 5% non-fat dairy milk added to each well for 3 h. After washing, europium-tagged anti-rabbit secondary antibody (0.5 μg/mL in 1% BSA/PBS; Perkin Elmer Life Sciences, Turku, Finland) was added and the plates incubated for 1 h at room temperature. After a final wash, Enhancement Solution (Perkin Elmer Life Sciences) was added, and time-resolved fluorescence was measured at excitation 355 nm and emission 620 nm using a FLUOstar Optima plate reader (BMG Labtek Australia). The collagen content of each sample was determined from the standard curve (μg/mL), constructed from purified type I human placental collagen (BD Biosciences Australia, North Ryde, NSW)

and then normalised to DMEM-only treated cells.

2.5. In vitro mineralization

Normal human bone-derived osteoblasts were seeded into 96-well plates (Nunc) at a density of 1.2×10^4 cells per well and cultured for 5 days in ascorbic acid-free (AA-free) 10% FBS/DMEM at 37 °C and 5% CO_2. Triplicate wells were stimulated with SBP in osteogenic DMEM mineralization medium [DMEM supplemented with 5% FBS, 100 μmol/L AA 2-phosphate (Wako Chemical Industries), 10^{-8} mol/L dexamethasone (Hospira Australia, Mulgrave, VIC), and 10 mmol/L β-glycerophosphate (Sigma-Aldrich)] to assist bone mineral formation. Cells were maintained in culture for 21 days, with fresh medium with or without SBP, changed every 7 days. To detect matrix mineralization, the Alizarin Red staining method was used as previously described (DeNichilo et al., 2016). Briefly, cells were washed with PBS and fixed with 10% buffered formalin. The fixed cells were then washed twice with distilled water and stained with 2% Alizarin Red S solution (Sigma-Aldrich). The stained mineralized matrix was photographed using a Nikon Eclipse 50i microscope attached to a DS-L2 control unit (Digital Sight, Nikon Europe, Amsterdam, The Netherlands) and a DS-Fi1 digital camera (Nikon Corporation, Tokyo, Japan).

The extent of mineralization was quantitated by eluting the Alizarin Red S dye with 10% (w/v) cetylpyridinium chloride (Sigma-Aldrich) in 10 mM phosphate buffer pH 7.0, for 10 mins to release remaining calcium-bound Alizarin Red S. Absorbance was measured at a wavelength of 570 nm using a FLUOstar Optima plate reader (BMG Labtek Australia).

2.6. Microarray

A microarray was performed to evaluate the effects of SBP on pro-osteogenic gene expression in primary human osteoblasts. Briefly, osteoblasts harvested from a single donor were seeded at a density of 6×10^4 into T25 culture flasks in 10%FBS/DMEM/ and maintained in culture for 5 days. On reaching confluence, cells were stimulated with or without 5 μg/mL SBP for 12 days in osteogenic DMEM mineralization medium. Total RNA was harvested using an RNeasy Mini Kit (Qiagen Australia, Chadstone, VIC) according to the manufacturer's instructions and used to probe the Illumina HT-12 microarray platform, targeting over 47,000 human transcripts (Australian Genome Research Facility, Parkville, VIC). The Illumina GenomeStudio software (Version 1.9.0) was used to extract and normalise the expression data for the mean intensity of the array. Genes that were statistically significant ($p = \leq 0.05$) and exceeded a pre-set threshold for significantly higher (≥1.5-fold change) or lower (≤1.5-fold change) expression compared to control were included for further analysis. Of the genes presented in the array, 836 genes met this prerequisite. Only those genes which had the greatest difference in fold change previously implicated in osteogenesis and repair were selected for validation using RT-PCR analysis. Functional pathways were analysed using the open web-based Database for Annotation, Visualisation and Integrated Discovery (DAVID) Bioinformatics Resources 6.7 (Da et al., 2009; Huang da et al., 2009) (Table 1). Microarray data (GSE168303) is available at https://www.ncbi.nlm.nih.gov/geo/query/acc.cgi?acc=GSE168303.

2.7. Quantitative real-time PCR (qRT-PCR)

To validate candidate osteogenic genes from the microarray, qRT-PCR was performed based on the above-mentioned conditions with SBP at 6.25 μg/mL. Custom TaqMan® Array Fast Plates (Thermo Fisher, Scoresby, VIC) were pre-spotted with TaqMan® Gene Expression Assay probes for *BMP-2*, *BSP*, *WNT-5A*, *FRZ—B*, *CCL5*, *CXCL5*, *CXCL6*, *CXCL12*, *MMP1*, *MMP3*, *IL6* and *IL8*. *GAPDH* was used as the control house-keeping gene. Quantitative RT-PCR was performed using TaqMan® Fast Advanced Master Mix (Thermo Fisher, Scoresby, VIC), in a ViiA 7 Real-Time System (Applied Biosystems, Foster City, CA).

Table 1
Pathways of genes differentially expressed by SBP-treated osteoblasts.

Term	Count	Genes	Fold enrichment
GO:0001503 ~ ossification	2	*BSP*, *BMP2*,	29.40
GO:0006954 ~ inflammatory response	5	*IL6*, *BMP2*, *IL8*, *CXCL6*, *CCL5*	18.92
GO:0006955 ~ immune response	6	*IL6*, *IL8*, *CXCL5*, *CXCL6*, *CXCL12*, *CCL5*	10.69
GO:0009611 ~ response to wounding	5	*IL6*, *BMP2*, *IL8*, *CXCL6*, *CCL5*	11.60
GO:0016477 ~ cell migration	4	*IL6*, *IL8*, *CXCL12*, *CCL5*	17.82
GO:0031012 ~ extracellular matrix	3	*WNT5A*, *MMP3*, *MMP1*	12.34

2.8. In vivo sheep model and surgery

The sheep ($n = 4$) were fasted for 12 h prior to surgery but had *ad libitum* access to water during this time. To alleviate post-operative pain, a fentanyl patch (2–3 μg/kg/h) was applied 24 h prior to surgery and reapplied every 72 h for a minimum of 10 days. After pre-emptive sedation and analgesia with midazolam (0.2 mg/kg) and buprenorphine (0.005 mg/kg), animals were anaesthetised with Propofol, which was administered until effect (3–4 mg/kg). Animals were then intubated and administered Isoflurane in oxygen at 2%. A patient warmer was used during the procedure to keep the animal's body temperature stable and to prevent hypothermia. The antibiotic, Cephalosporin (22 mg/kg) and anti-inflammatory, Meloxicam (0.2 mg/kg) were administered pre-emptively and during the surgical procedure. Non-steroidal anti-inflammatory flunixin meglumine (1.1 mg/kg) was also administered. Animals were positioned in dorsal recumbency and the operative site for each hind limb was prepared through sequential sterilising scrubs and draping.

2.9. Femoral condyle implantation

A veterinary surgeon marked and created a 2–3 cm incision, directly over the mid-medial aspect of the femoral condyle, revealing the underlying soft tissue which was separated to expose the bone. A 12 mm diameter, 10 mm deep defect was then created with sequential use of differing size drill heads. This method was used to avoid unnecessary thermal necrosis. The defect was then flushed with saline to remove any remaining bone fragments. Once the defect was created, commercially available BCP [15% HA/85% β-TCP] granules (Medtronic Sofamor Danek, Memphis, TN) were prepared for treatments and deposited into the condyle defect. In one defect, 1.25 g BCP, which was pre-soaked for 15 mins in 5 mL soybean peroxidase (650 μg/mL) was added. The other defect received 1.25 g BCP pre-soaked with 5 mL saline (Hartmann's solution, Baxter Healthcare, Coparoo, QLD) solution as the control. It is important to note that the total amount of SBP was fully absorbed into the BCP granules which were then gently compacted into the defect to ensure consistent and even distribution. The wound was closed using 0-vicryl in a cruciate pattern for the deep fascial layer and continuous pattern for the subcutaneous layer. Metallic skin staples were then applied over the surface. Finally, a bandage with antimicrobial dressing was applied over the surgical site. Animals remained in a sling for 24 h before being moved to indoor housing for the entirety of the study. The animals were sacrificed 4 weeks post-surgery and specimens were obtained by aseptic technique.

2.10. Microcomputed tomography (micro-CT) imaging

Samples in 70% ethanol were cut to size in order to fit within a 36.9 mm diameter sample tube with the drill hole defect in vertical

orientation. The samples were scanned in a micro-CT scanner 40 (Scanco Medical, Bassersdorf, Switzerland) at an energy of 70 kV and intensity of 114 μA with 200 μs integration time, resulting in an isotropic voxel size of 36 μm. The reconstructed scans were evaluated using Scanco μCT Evaluation Program (v6.5–3). A cylindrical volume of interest (VOI) with a diameter of 11 mm was defined for the analysis. The vertical evaluation length (cylinder height) was defined in a preview and consisted of the central, cylindrical section of the defect (approximately 100 slices or 3.6 mm), excluding the zones at the top and bottom ends of the defect to prevent "boundary effects." To identify newly formed bone throughout the VOI, and to reduce partial volume effect at the grain boundaries of the ceramic granules, a masking procedure was employed (Burghardt et al., 2008). First, using a high threshold of 5069 Hounsfield Units (HU, 872.6 mg HA/mm^3), with a gauss filter of $\sigma = 0.8$ and a support of 1.0 was applied to segment the BCP granules within the defect. Next, the granules were enlarged by 2 voxels on all faces, and this enlarged granule volume was deducted from the VOI, leaving only the intra-granule space of the VOI. Newly formed bone was segmented from this space with a lower threshold of 2121 HU (356.3 mg HA/mm^3), a gauss filter of $\sigma = 1.8$ and a support of 3.0. For the quantitative evaluation, the total cylindrical volume of interest (TV), the volume of the segmented newly formed bone (BV) and the average mineral density of the newly formed bone were calculated.

2.11. Histology and histomorphometric analysis

Femoral condyles were subjected to ethanol dehydration steps prior to being placed into a Methyl Methacrylate (MMA): Polyethylene Glycol 400 (PEG) solution (100% MMA: 10% PEG). Femura were left in the MMA: PEG solution for 21 days, at which time polymerisation was induced using a solution containing MMA: PEG: Perkadox (0.2%). Trimmed resin blocks were sectioned in the sagittal plane at 10 μm thickness. Sections were prepared for Toluidine Blue (1% sodium tetraborax) and Tartrate Resistant Acid Phosphatase (TRAP) staining and counterstained with hematoxylin as previously described (Arthur et al., 2013). The stains were visualised with the Olympus BX53F microscope and imaged using the Olympus DP74 camera. Two dimensional histomorphometric analysis of the femoral condyles were performed using OsteoMeasure™ software (OsteoMetrics, Decatur, USA) as previously described (Nguyen et al., 2016), where the assessor was blinded to the sample identity.

2.12. Statistical analysis

Data points derived from experiments are reported as the mean ± standard error of the mean (SEM). Analysis of variance to determine the significant difference between samples was performed using the paired two-tailed Student's *t*-test on GraphPad Prism 8 Version 8.4.1 for Windows (GraphPad Prism Software, San Diego, CA).

3. Results

3.1. SBP stimulates osteoblast collagen type I secretion

Collagen type I is the most abundant protein in bone and accounts for approximately 90% of the organic matrix in bone (Feng, 2009). When stimulated with increasing concentrations of SBP, in the absence of AA for 72 h, primary human osteoblasts displayed a dose-responsive increase in collagen type I release. Maximal doses of SBP resulted in a three-fold increase in soluble collagen type I release which was comparable to the amount measured in the presence of ascorbic acid (AA), which was used as the positive control (Fig. 1A). Notably, a significant increase in collagen type I secretion was observed at the lowest dose of SBP of 1.5 ng/mL. Assessment of cell viability indicated that SBP and AA had no impact on osteoblast numbers (Fig. 1B). This confirmed that SBP is non-toxic at the doses tested and importantly, shows the increase in collagen type I was not related to effects on cellular proliferation., These results demonstrate that the plant-derived SBP can promote collagen type I secretion by osteoblasts in an ascorbic acid-independent manner, consistent with previous studies of mammalian peroxidases (DeNichilo et al., 2016).

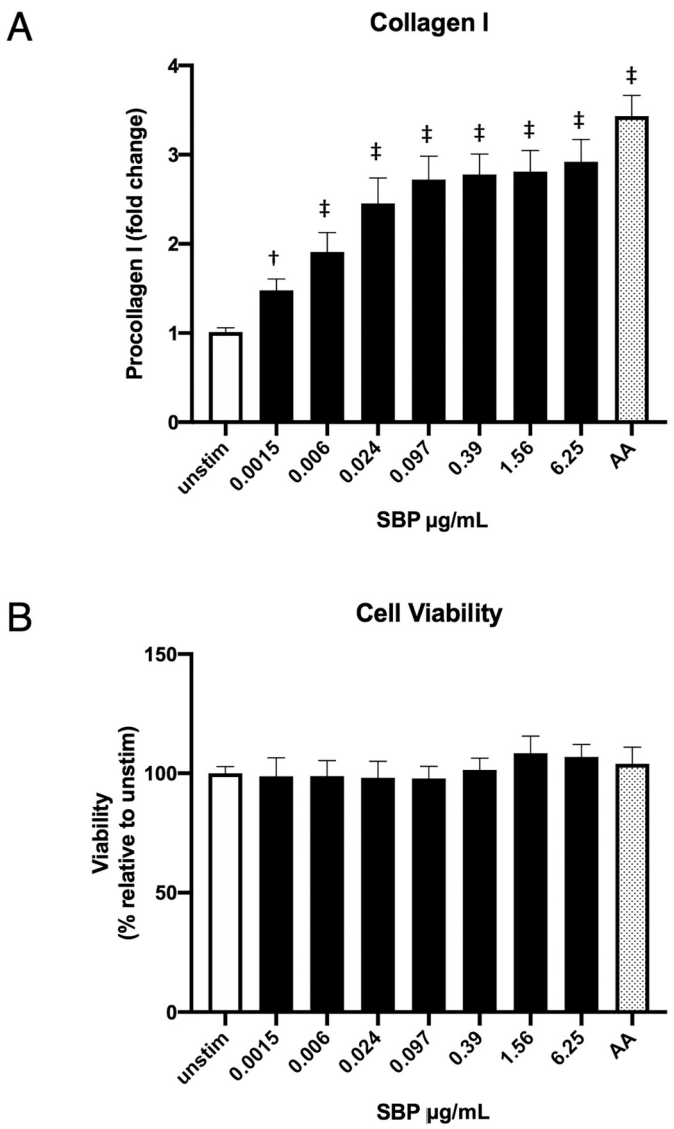

Fig. 1. *SBP promotes collagen I release by cultured human osteoblasts.* **(A)** ELISA detection of soluble collagen I in osteoblast-conditioned medium after 72 h stimulation with SBP at the doses indicated. Ascorbic acid 2-phosphate (AA) at 100 μmol/L served as the positive control, whereas cells treated with Dulbecco's modified Eagle's medium (DMEM) alone (unstim) served as the baseline control. The levels of collagen I are expressed as fold change and normalised to the unstim control. The data are pooled from three separate donors performed in triplicate. **(B)** Viability of cultured osteoblasts after 72 h stimulation as assessed using the alamarBlue dye assay. Cell viability was normalised, so the average values of unstim cells were set to 100% relative to each peroxidase dose. The data are pooled from three experiments each conducted using cells derived from three donors. Data are the mean ± SEM for unstim, AA, and each peroxidase dose. (†$P < 0.01$; ‡$P < 0.001$).

3.2. SBP stimulates osteoblast matrix mineralization in vitro

To determine whether SBP could also influence matrix mineralization *in vitro*, primary human osteoblasts were cultured in increasing concentrations of SBP up to 12.5 μg/mL in the presence of DMEM

mineralization media for 21 days. Osteoblasts cultured with SBP produced more calcium deposits relative to vehicle control (Unstim) in a dose-dependent manner, based on Alizarin Red staining (Fig. 2A). Quantification of the eluted Alizarin Red S dye revealed that the stimulation of SBP resulted in a significant increase in mineralization from 1.6-fold at the lowest dose (0.78 μg/mL) up to 4-fold increase at the highest doses (from 3.25 to 12.5 μg/mL) compared to no SBP (Unstim) (Fig. 2B). Together, these data suggest that SBP promotes matrix mineralization of stimulated primary human osteoblasts.

Furthermore, to investigate the capacity of SBP to perform as an osteoinductive agent *in vivo*, we evaluated human osteoblast migration and mineralization in a three-dimensional collagen scaffold presoaked with or without SBP. These supportive *in vitro* studies suggest that SBP stimulates osteoblast matrix infiltration after 14 days (Supp. Fig. 1A) and may enhance matrix mineralization after 28 days (Supp. Fig. 1B).

3.3. SBP regulates expression of genes involved in osteoblast function

Next, we sought to determine the changes in osteoblast gene expression mediated by SBP. To this end, we performed a RNA microarray on SBP-treated osteoblasts which identified 6554 genes that where differentially expressed, of which, 12 key genes involved in osteoblast function and regeneration were identified. Using web-based classification programs (as described in the Methods), the differentially expressed genes were characterised into six categories: those involved in ossification, inflammatory and immune responses, cell migration, extracellular matrix and genes expressed in response to healing (Table 1). The qRT-PCR analysis confirmed the microarray gene expression profile for *BMP-2*, *BSP*, *WNT-5A*, *FRZ—B*, *CCL5*, *CXCL5*, *CXCL6*, *CXCL12*, *MMP1*, *MMP3*, *IL-6 and IL-8* (Fig. 3). Taken together, these results suggest that peroxidases act by stimulating the differential regulation of effector genes that are key to osteogenesis and repair.

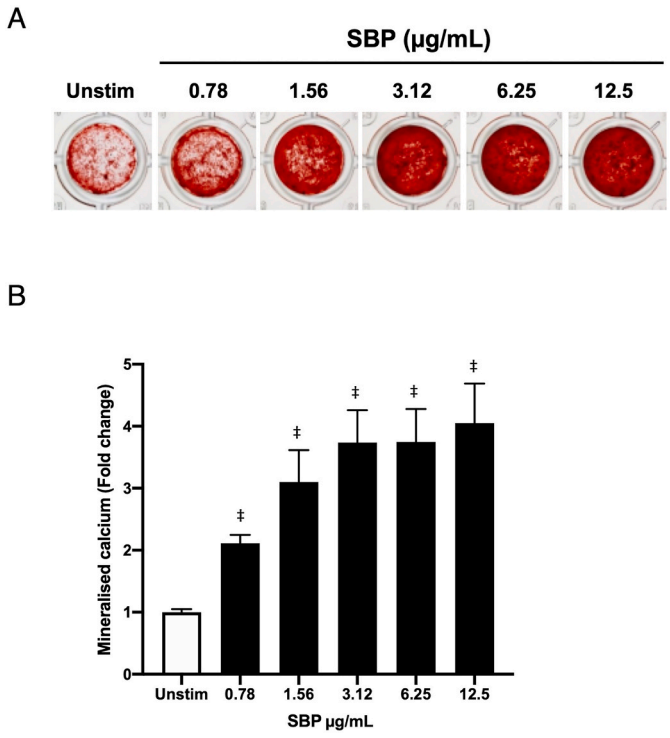

Fig. 2. *SBP promotes osteoblast matrix mineralization in vitro.* **(A)** Representative images of Alizarin Red stained cultured human osteoblasts stimulated with SBP for 21 days at the various doses indicated. **(B)** Quantitation of mineralized calcium extracted from cultured osteoblast monolayers following stimulation with SBP for 21 days at the doses indicated. Cells treated with mineralization medium alone (unstim.) served as the baseline control. The levels of mineralized calcium are normalised to the unstim control and expressed as fold change. Statistical significance was calculated by two-tailed Student's *t*-test with the various doses of SBP compared to the mineralization medium alone (unstim) group. Data are the mean ± SEM of three independent donors. (‡$P < 0.001$).

3.4. SBP promotes bone regeneration of critical size defects in the long bones of sheep

Ovine models have been used extensively to model human bone structure and bone metabolism and to investigate various osteoinductive factors (Field et al., 2011; Field et al., 2009). To demonstrate the efficacy of SBP-targeted fracture therapy, we used a SBP concentration of 650 μg/mL delivered on BCP granules to treat a standardized bilateral femoral drill-hole defect (Supp. Fig. 2A). Saline and SBP-soaked BCP granules were prepared and implanted directly into the defect site (Supp. Fig. 2B). No surgical complications or postoperative morbidities were reported. Using micro-CT imaging and analysis, the effect of SBP in combination with BCP granules on bone formation after 4 weeks of implantation was evaluated. Representative three-dimensional reconstructions of the micro-CT images encompassing the central zone of the defect (Fig. 4A) showed that SBP treatment increased bone formation compared to saline control (Fig. 4B). Quantitative analysis of the reconstructions revealed a statistically significant 2.7-fold increase in bone to tissue volume at the defect site in the SBP-treated limbs compared to saline control (Fig. 4C).

Histological analysis of the defect sites was performed on sections stained with toluidine blue to identify new bone formation and osteoblasts, whereas TRAP staining was used to identify the osteoclast population (Fig. 5A–B). Two dimensional double-blinded histomorphometric assessment through the mid-region, relative to depth of the defect suggested that the presence of SBP promoted new bone formation when compared to control although, this did not reach statistical significance ($p = 0.054$) (Fig. 5C). This observation correlated with a decrease in the amount of granule area relative to tissue volume at the defect margins that was not due to changes in fibrous tissue volume. Furthermore, while not reaching statistical significance, SBP stimulated an associated increase in trabecular number and number of osteoblasts. TRAP staining of the defect site suggested that while SBP did not influence osteoclast formation, or number, osteoclasts were found to aggregate at the boundary between the granule and the newly mineralizing fibrous tissue. This is consistent with the bone remodelling process where osteoclasts are present and important during the resorption phase, remodelling the injury site and mostly devoid during the reversal stage, which prepares for a permissive bone forming environment. Collectively this data supports the *in vitro* and micro-CT three dimensional findings that SBP enhances bone formation and potentially promotes/supports infiltration of osteogenic precursors into the defect area.

4. Discussion

Bone repair following injury or disease is a highly coordinated and complex process that involves the interplay of numerous cell types, and their extracellular matrix components. Recruited to the injury site from the surrounding tissue, osteoblasts have central role for the synthesis and deposition of a collagen-rich extracellular matrix (ECM) that subsequently mineralizes to form bone. Circulating inflammatory cells, including neutrophils, eosinophils and macrophages, infiltrate the fracture site during the early inflammatory phase of this bone healing process (Andrew et al., 1994; Claes et al., 2012; Prasad and Udupa, 1972), where they release pro-osteogenic factors locally that influence osteoblast recruitment, functionality and the regenerative process. Peroxidases are heme-containing enzymes are also released in abundance at sites of injury and inflammation by the infiltrating immune cells and, until recently, their functional role was thought to be limited to providing oxidative defence against invading bacteria and other

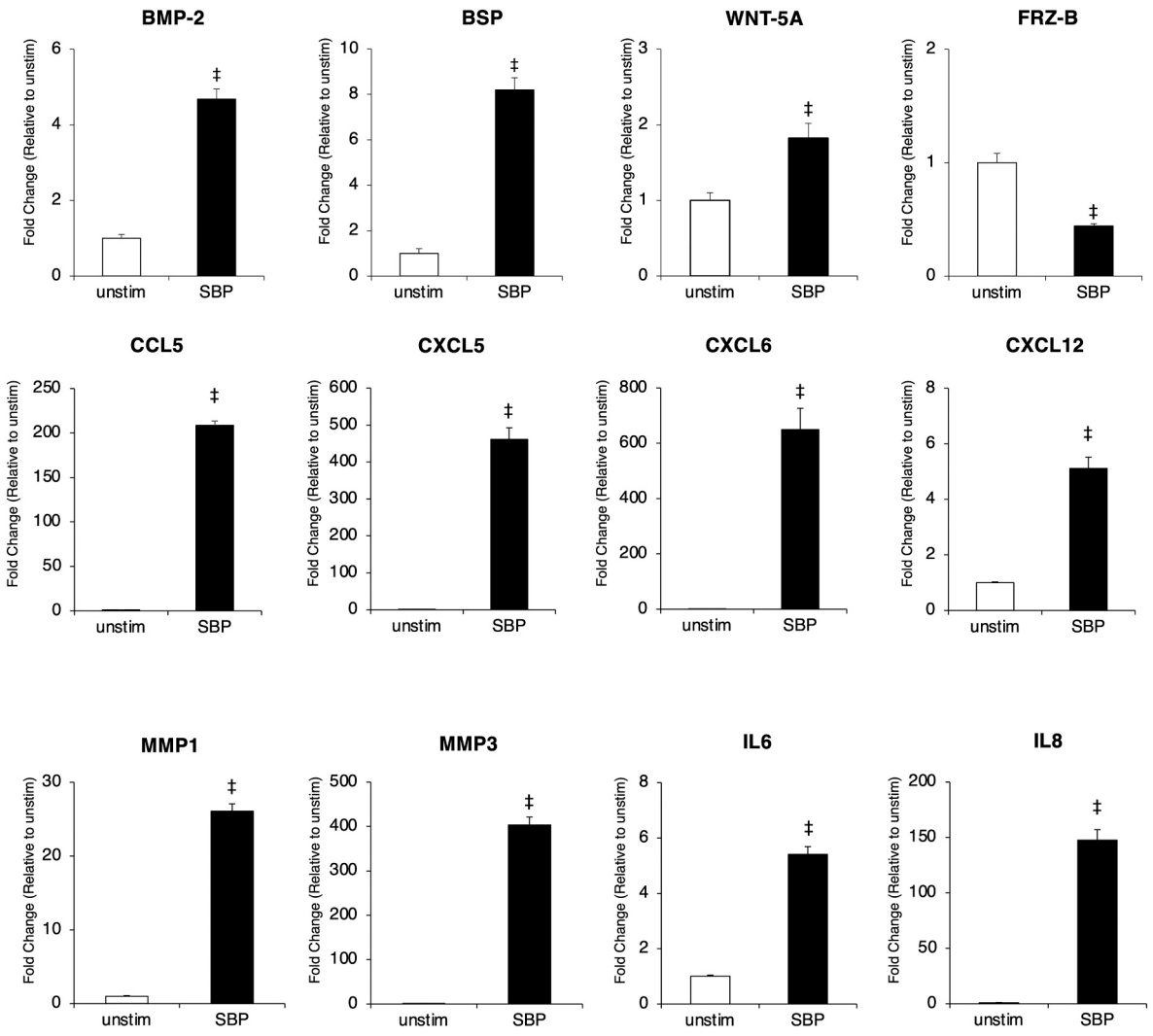

Fig. 3. *SBP regulates osteogenic gene expression.* Quantitative real-time PCR analysis of the *BMP-2*, *WNT-5A*, *BSP*, *FRZ—B*, *CCL6*, *CXCl12*, *IL-6*, and *MMP1* mRNA expression (normalised to *GAPDH*) in cultured osteoblasts following stimulation with 6.25 μg/mL soybean peroxidase (SBP) for 12 days. Cells treated with DMEM mineralization medium (unstim) served as the baseline control. Transcript levels were normalised to and expressed as fold change relative to the unstim control. Statistical significance was calculated by two-tailed Student's *t*-test with the SBP treatment group compared to unstim. Data are the mean ± SD of triplicate determinations. (†$P < 0.01$; ‡$P < 0.001$).

pathogenic microorganisms. However, we have recently uncovered prominent and previously unrecognised roles for this group of enzymes in bone biology that has great potential as a therapy for bone repair. Our previous studies revealed that mammalian peroxidases, including MPO and EPO, as well as plant derived peroxidase proteins, such as HRP and SBP, regulate fibroblast collagen extracellular matrix biosynthesis (DeNichilo et al., 2015), regulate collagen biosynthesis and matrix mineralization by human osteoblasts (DeNichilo et al., 2016), inhibit osteoclast differentiation and bone resorption (Panagopoulos et al., 2017b) and drive angiogenesis (Panagopoulos et al., 2015). These biological processes are intimately involved in the pathway to bone repair. Until now the use of a peroxidase enzyme to therapeutically promote bone regeneration *in vivo* has never been contemplated or demonstrated. In the present study, we investigated the effect of the plant-derived SBP in regulating bone matrix formation *in vitro* and bone ossification *in vivo* as a potential osteoinductive agent.

Collagen type I is the major extracellular matrix constituent of bone and its synthesis by osteoblasts is critical for normal bone formation (Cox et al., 2010). We report here for the first time, that SBP stimulates collagen I release by human osteoblasts in the absence of AA supplementation akin to its mammalian family of peroxidase enzymes, MPO and EPO (DeNichilo et al., 2015). However, unlike MPO and EPO, SBP was found to be more potent at inducing a collagen response at much lower concentrations, indicative of its greater enzymatic catalytic activity (DeNichilo et al., 2015). The role of AA in ECM production has been well characterised, by its ability to promote hydroxylation of peptidyl-proline which results in the assembly of a stabilised triple-helical procollagen molecule, subsequently leading to a collagen-rich matrix that is able to become mineralized (Franceschi and Iyer, 1992). In addition to stimulating an increase in collagen type I, we demonstrate that increasing concentrations of SBP, significantly increased the mineralization rate when compared to AA alone. Bone matrix mineralization is the final stage of ossification leading to the formation of new bone. These results suggest that the composition of the collagen fibrils induced by SBP are indeed appropriate to ensue mineral accumulation, while also enhancing the bone mineralization process when cultured in osteogenic media. The interaction between osteoblasts and organic matrix components plays a critical role on cell differentiation, survival, proliferation, and matrix mineralization (Feng, 2009). In this regard, we show *in vitro* that after two weeks of culture, SBP promotes osteoblast infiltration into a collagen-rich three-dimensional scaffold (INTEGRA®) and a concomitant increase in matrix mineralization after just four

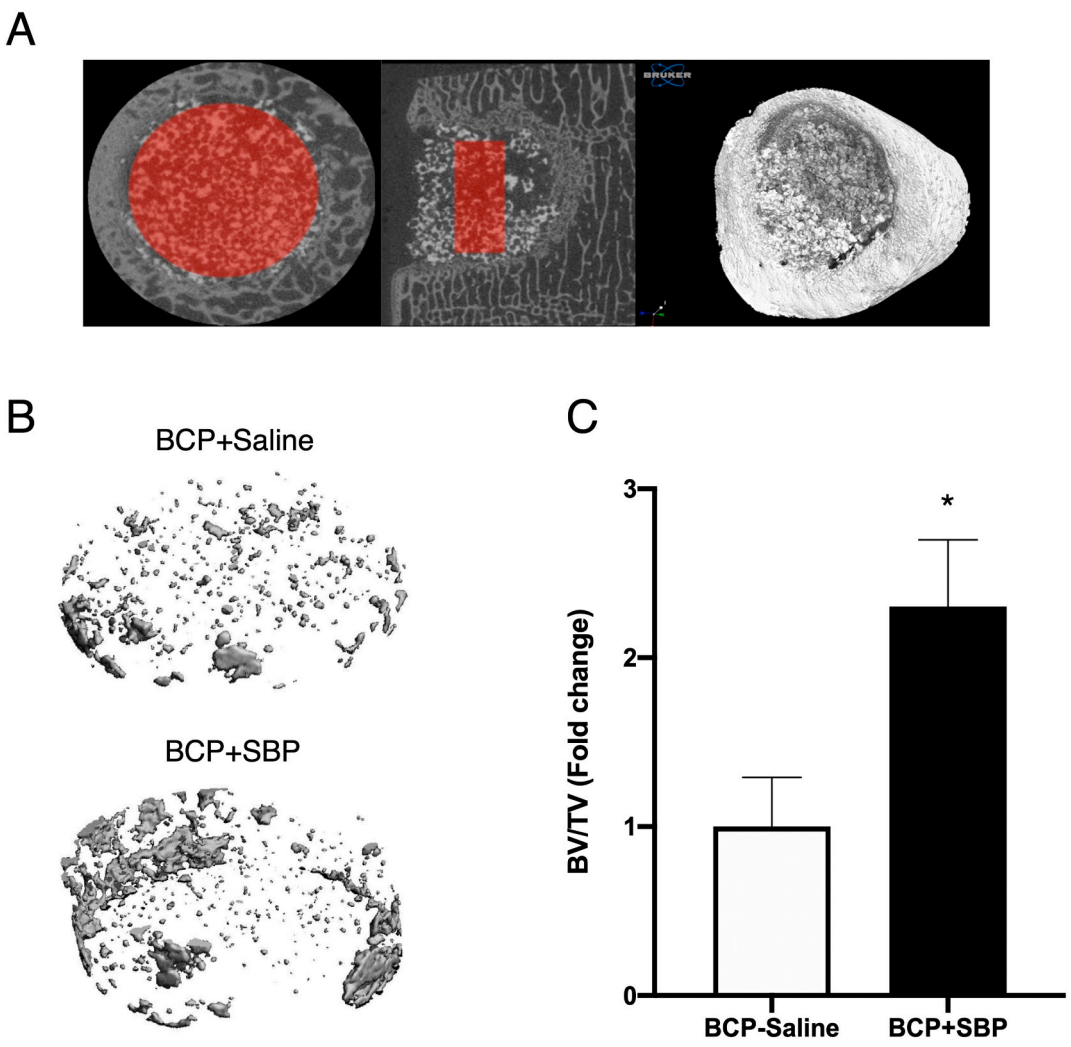

Fig. 4. *Localised application of SBP-soaked BCP granules within a femoral defect increases bone formation.* (A) Representative micro-CT image of reconstructed defect block used for quantification. A cylindrical volume of interest (VOI) with a diameter of 11 mm and length of 3.6 mm. **(B)** Representative micro-CT reconstructions of the defect site 28 days post-transplantation. **(C)** Quantitative analysis of the mean bone volume (BV) to tissue volume (TV) of the SBP treatment compared to BCP + saline control within the defect site. Data was analysed and reported as the mean ± SEM. Analysis of variance to determine significant difference between samples was performed using the paired Student's *t*-test of four sheep for control and peroxidases. (*$P < 0.05$).

weeks. These studies provided important information to explore the effects of SBP on bone formation *in vivo*.

Mechanistically, our analysis of global gene expression shows that SBP is an effective regulator of several well-characterised genes known to be involved in osteoblast functions including, differentiation, mineralization and repair. However, an important limitation of this preliminary finding is that only one biological replicate was analysed. Using qRT-PCR validation we showed that SBP significantly up-regulated *BMP-2*, *BSP* and *WNT-5A* osteogenic signature genes. BMP-2 is an important regulator in osteogenesis and it has been shown to drive BSP and WNT-5A expression by cultured osteoblasts (Lecanda et al., 1997; Robubi et al., 2014). Conversely, SBP down-regulates a known repressor of osteogenesis, FRZ-B related protein. FRZ-B acts as a competitive inhibitor of the WNT signalling pathway (Cho et al., 2008) which, like BMP-2 is a key modulator of bone formation (Takada et al., 2009). These data suggest that SBP may, in part, promote intramembranous ossification *via* induction of BMP-2, which acts as an intermediate for the regulation of downstream effector genes. BMP-2 has been extensively tested both *in vitro* and *in vivo* as an agent for the repair of osseous defects both alone and in combination with other growth factors and biomaterials (Nakamura et al., 2005; Simmons et al., 2004; Street et al., 2002). While BMP-2 appears to be the most potent osteoinductive agent identified to-date, several studies have shown osteoclastic activation and bone resorption in response to BMP-2 treatment (Seeherman et al., 2010; Toth et al., 2009), which may interfere with accelerated bone repair, supporting the notion that other biological factors are urgently required.

In addition to the regulation of genes involved in osteoblast function by SBP, we observed significant up-regulation of numerous cytokines and chemokines including CCL5, IL-6, and CXCL12, which are crucial in the recruitment and regulation of bone remodelling. For example, CCL5 is suggested to play a crucial role in osteoblast migration and survival *in vitro* (Yu et al., 2004), while in a knockout mouse model, bone formation was significantly impaired with an observed increase in osteoclastogenesis (Wintges et al., 2013). The pro-inflammatory cytokine IL-6 has been shown to enhance and inhibit osteoclastogenesis and more recently reported to be involved in promoting osteoclastogenesis by indirectly increasing RANKL expression by osteoblasts (Duplomb et al., 2008; Udagawa et al., 1995). Up-regulated CXCL12 is also involved in bone formation and healing. Previous studies have shown that blocking CXCL12 or its receptor CXCR4, led to reduced expression/function? of osteoblastic transcription factors and differentiation markers (Zhu et al., 2007). Furthermore, in a mouse model, inactivation of CXCR4 resulted in reduced bone mass, decreased bone mineral density and decreased

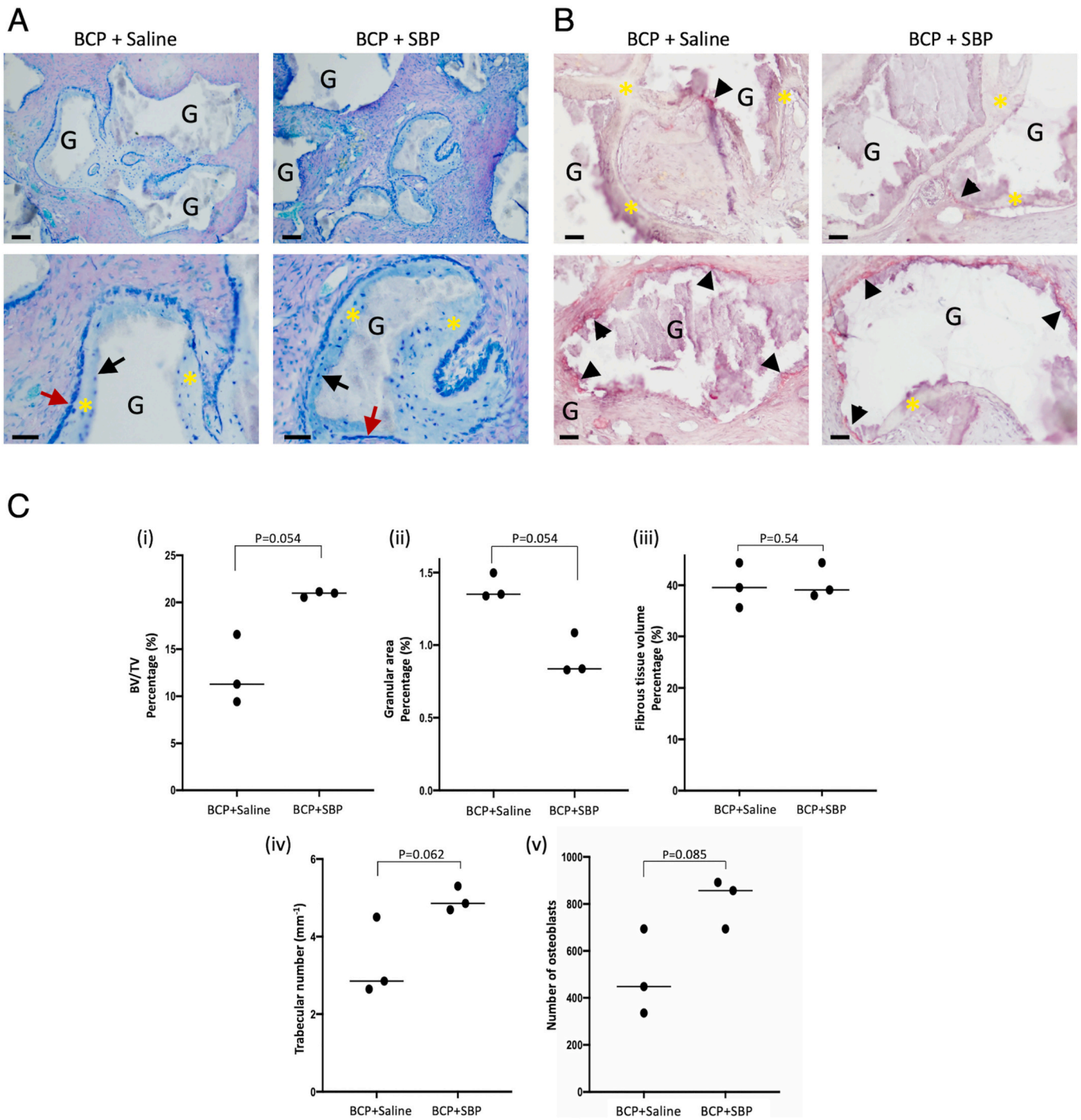

Fig. 5. *Histomorphometric analysis suggests SBP treatment enhances bone formation in a in vivo bone defect model.* (A–B) Representative **(A)** toluidine blue and **(B)** TRAP stained sections of the sheep femoral defect treated with saline (MG + saline) or SBP-soaked (MG + SBP) HA/β-TCP Mastergraft® (MG) BCP granulesafter 28 days. **(C)** Histomorphometric analysis of the defect site represented as the (i) percentage of tissue volume to bone volume, (ii) percentage of granular area, (iii) percentage of fibrous tissue volume relative to tissue volume, (iv) trabecular number, and (v) number of osteoblasts. All statistical analysis was performed by a paired Student *t*-test, $n = 3$ animals. (Yellow asterisks = bone formation adjacent to BCP granules. "G" = location of MG granules. Red arrows = osteoblasts (dark blue) lining the new bone forming surface. Black arrows = embedded osteocytes (dark blue/ pale purple). Arrow heads = osteoclasts. Scale bar A-B = 50 μm). Statistical significance was calculated by two-tailed Student's *t*-test with the SBP treatment group compared to unstim. Data are the mean ± SD of triplicate determinations.

expression of collagen type I (Zhu et al., 2011).

The ability of SBP to influence the mineralization process beyond the initial stage of collagen biosynthesis and the regulation of key osteogenic genes suggests that SBP possesses the necessary properties to induce osteogenic repair. To test this hypothesis, we utilised the critical-sized bone defect (CSD) model in sheep in combination with BCP serving as a scaffold, which is the 'gold standard' approach in evaluating new treatment modalities for bone repair or regeneration with similar bone metabolism to humans (Apelt et al., 2004; Theiss et al., 2005; Patel et al., 2005). This hypothesis is further supported by our previous findings whereby SBP was found to induce connective tissue regeneration and intergration of a three-dimensional dermal regeneration scaffold in a

porcine full-thickness wound model (DeNichilo et al., 2015). The critical-sized femoral condyle defect model described herein, showed new bone formation and integration after 4 weeks of BCP implantation. Notably, the SBP soaked BCP implant significantly increased bone regeneration by 2-fold when compared to BCP alone as shown by micro-CT. Our blinded histomorphometry analysis of the tissue specimens validate the observed micro-CT results. In the SBP group, increased bone volume accounted for approximately 21% of the defect area, while in vehicle group the bone volume level was 12% which was almost a 2-fold difference. In addition to the increase in trabecular volume, it is evident that the presence of SBP promoted an increase in osteoblast infiltration and an overall increase in bone area. However, at the single 4 week time point, we observed no difference in the vessel (data not shown) or osteoclast number in either group, contrary to our previous findings showing peroxidase mediated increase in vascularisation and inhibition of osteoclastogenesis (Panagopoulos et al., 2015; Panagopoulos et al., 2017a). Taken together, this study has demonstrated an ability for SBP to promote new bone formation without any apparent toxicity to the local cell population, where we see an abundance of osteoblasts and osteocytes, necessary for normal bone healing.

In conclusion, our findings demonstrate for the first time, a pro-osteogenic role for SBP, by its ability to promote collagen I biosynthesis and matrix mineralization and shows promising potential as a new and cost-effective therapeutic able to promote bone repair *in vivo*.

CRediT authorship contribution statement

Alexandra J. Barker: Investigation, Visualization, Writing – original draft. **Agnes Arthur:** Investigation, Formal analysis. **Mark O. DeNichilo:** Investigation, Methodology. **Romana Panagopoulos:** Investigation. **Stan Gronthos:** Resources, Writing – review & editing. **Peter J. Anderson:** Supervision, Writing – review & editing. **Andreas Evdokiou:** Resources, Writing – review & editing. **Vasilios Panagopoulos:** Conceptualization, Supervision, Writing – review & editing.

Declaration of competing interest

The authors declare that they have no competing interests.

Acknowledgements

The authors would like to acknowledge Dr. John Field for his surgical expertise, Dr. Roland Steck and QUT MERF for their analytical support, and Ms. Shelley Hay and Ms. Rebecca Sawyer for their technical assistance. This work was supported in part by The Hospital Research Foundation, Adelaide Research and Innovation Commercial Accelerator Scheme and the National Health and Medical Research Council (Career Development Fellowship/627015; Project Grant/1050694). V·P was supported by an NHMRC Early Career Fellowship (APP1160000).

Appendix A. Supplementary data

Supplementary data to this article can be found online at https://doi.org/10.1016/j.bonr.2021.101096.

References

Almaiman, M., Al-Bargi, H.H., Manson, P., 2013. Complication of anterior iliac bone graft harvesting in 372 adult patients from may 2006 to may 2011 and a literature review. Craniomaxillofac. Trauma Reconstr. 6 (4), 257–266.

Andrew, J.G., Andrew, S.M., Freemont, A.J., Marsh, D.R., 1994. Inflammatory cells in normal human fracture healing. Acta Orthop. Scand. 65 (4), 462–466.

Apelt, D., Theiss, F., El-Warrak, A.O., Zlinszky, K., Bettschart-Wolfisberger, R., Bohner, M., Matter, S., Auer, J.A., von Rechenberg, B., 2004. In vivo behavior of three different injectable hydraulic calcium phosphate cements. Biomaterials 25 (7–8), 1439–1451.

Arthur, A., Panagopoulos, R.A., Cooper, L., Menicanin, D., Parkinson, I.H., Codrington, J. D., Vandyke, K., Zannettino, A.C., Koblar, S.A., Sims, N.A., Matsuo, K., Gronthos, S., 2013. EphB4 enhances the process of endochondral ossification and inhibits remodeling during bone fracture repair. J. Bone Miner. Res. 28 (4), 926–935.

Aruoma, O.I., Halliwell, B., 1987. Action of hypochlorous acid on the antioxidant protective enzymes superoxide dismutase, catalase and glutathione peroxidase. Biochem. J. 248 (3), 973–976.

Atkins, G.J., Kostakis, P., Pan, B., Farrugia, A., Gronthos, S., Evdokiou, A., Harrison, K., Findlay, D.M., Zannettino, A.C., 2003. RANKL expression is related to the differentiation state of human osteoblasts. J. Bone Miner. Res. 18 (6), 1088–1098.

Betz, R.R., 2002. Limitations of autograft and allograft: new synthetic solutions. Orthopedics 25 (5 Suppl), s561–s570.

Bouler, J.M., Pilet, P., Gauthier, O., Verron, E., 2017. Biphasic calcium phosphate ceramics for bone reconstruction: a review of biological response. Acta Biomater. 53, 1–12.

Burghardt, A.J., Kazakia, G.J., Laib, A., Majumdar, S., 2008. Quantitative assessment of bone tissue mineralization with polychromatic micro-computed tomography. Calcif. Tissue Int. 83 (2), 129–138.

Cho, S.W., Her, S.J., Sun, H.J., Choi, O.K., Yang, J.Y., Kim, S.W., Kim, S.Y., Shin, C.S., 2008. Differential effects of secreted frizzled-related proteins (sFRPs) on osteoblastic differentiation of mouse mesenchymal cells and apoptosis of osteoblasts. Biochem. Biophys. Res. Commun. 367 (2), 399–405.

Claes, L., Recknagel, S., Ignatius, A., 2012. Fracture healing under healthy and inflammatory conditions. Nat. Rev. Rheumatol. 8 (3), 133–143.

Cox, G., Einhorn, T.A., Tzioupis, C., Giannoudis, P.V., 2010. Bone-turnover markers in fracture healing. J Bone Joint Surg Br 92 (3), 329–334.

Da, W. Huang, Sherman, B.T., Lempicki, R.A., 2009. Bioinformatics enrichment tools: paths toward the comprehensive functional analysis of large gene lists. Nucleic Acids Res. 37 (1), 1–13.

DeNichilo, M.O., Panagopoulos, V., Rayner, T.E., Borowicz, R.A., Greenwood, J.E., Evdokiou, A., 2015. Peroxidase enzymes regulate collagen extracellular matrix biosynthesis. Am. J. Pathol. 185 (5), 1372–1384.

DeNichilo, M.O., Shoubridge, A.J., Panagopoulos, V., Liapis, V., Zysk, A., Zinonos, I., Hay, S., Atkins, G.J., Findlay, D.M., Evdokiou, A., 2016. Peroxidase enzymes regulate collagen biosynthesis and matrix mineralization by cultured human osteoblasts. Calcif. Tissue Int. 98 (3), 294–305.

Duplomb, L., Baud'huin, M., Charrier, C., Berreur, M., Trichet, V., Blanchard, F., Heymann, D., 2008. Interleukin-6 inhibits receptor activator of nuclear factor kappaB ligand-induced osteoclastogenesis by diverting cells into the macrophage lineage: key role of Serine727 phosphorylation of signal transducer and activator of transcription 3. Endocrinology 149 (7), 3688–3697.

Feng, X., 2009. Chemical and biochemical basis of cell-bone matrix interaction in health and disease. Curr. Chem. Biol. 3 (2), 189–196.

Field, J.R., McGee, M., Wildenauer, C., Kurmis, A., Margerrison, E., 2009. The utilization of a synthetic bone void filler (JAX) in the repair of a femoral segmental defect. Veterinary and comparative orthopaedics and traumatology : V.C.O.T 22 (2), 87–95.

Field, J.R., McGee, M., Stanley, R., Ruthenbeck, G., Papadimitrakis, T., Zannettino, A., Gronthos, S., Itescu, S., 2011. The efficacy of allogeneic mesenchymal precursor cells for the repair of an ovine tibial segmental defect. Veterinary and comparative orthopaedics and traumatology : V.C.O.T 24 (2), 113–121.

Fillingham, Y., Jacobs, J., 2016. Bone grafts and their substitutes. Bone Joint J 98-B (1 Suppl A), 6–9.

Finkemeier, C.G., 2002. Bone-grafting and bone-graft substitutes. J. Bone Joint Surg. Am. 84 (3), 454–464.

Franceschi, R.T., Iyer, B.S., 1992. Relationship between collagen synthesis and expression of the osteoblast phenotype in MC3T3-E1 cells. J. Bone Miner. Res. 7 (2), 235–246.

Gamradt, S.C., Lieberman, J.R., 2003. Bone graft for revision hip arthroplasty: biology and future applications. Clin Orthop Relat Res (417), 183–194.

Gronthos, S., Mankani, M., Brahim, J., Robey, P.G., Shi, S., 2000. Postnatal human dental pulp stem cells (DPSCs) in vitro and in vivo. Proc. Natl. Acad. Sci. U. S. A. 97 (25), 13625–13630.

Helm, G.A., Dayoub, H., Jane Jr., J.A., 2001. Bone graft substitutes for the promotion of spinal arthrodesis. Neurosurg. Focus. 10 (4), E4.

Henriksen, A., Mirza, O., Indiani, C., Teilum, K., Smulevich, G., Welinder, K.G., Gajhede, M., 2001. Structure of soybean seed coat peroxidase: a plant peroxidase with unusual stability and haem-apoprotein interactions. Protein Sci. 10 (1), 108–115.

Hiraga, S., Sasaki, K., Ito, H., Ohashi, Y., Matsui, H., 2001. A large family of class III plant peroxidases. Plant Cell Physiol 42 (5), 462–468.

Homma, Y., Zimmermann, G., Hernigou, P., 2013. Cellular therapies for the treatment of non-union: the past, present and future. Injury 44 Suppl 1, S46–S49.

Huang da, W., Sherman, B.T., Lempicki, R.A., 2009. Systematic and integrative analysis of large gene lists using DAVID bioinformatics resources. Nat. Protoc. 4 (1), 44–57.

James, A.W., LaChaud, G., Shen, J., Asatrian, G., Nguyen, V., Zhang, X., Ting, K., Soo, C., 2016. A review of the clinical side effects of bone morphogenetic Protein-2. Tissue Eng Part B Rev 22 (4), 284–297.

Jimi, E., Hirata, S., Osawa, K., Terashita, M., Kitamura, C., Fukushima, H., 2012. The current and future therapies of bone regeneration to repair bone defects. Int J Dent 2012, 148261.

Kivrak, N., Taş, A.C., 1998. Synthesis of calcium hydroxyapatite-tricalcium phosphate (HA-TCP) composite bioceramic powders and their sintering behavior. J. Am. Ceram. Soc. 81 (9), 2245–2252.

Lecanda, F., Avioli, L.V., Cheng, S.L., 1997. Regulation of bone matrix protein expression and induction of differentiation of human osteoblasts and human bone marrow stromal cells by bone morphogenetic protein-2. J. Cell. Biochem. 67 (3), 386–396.

Nakamura, Y., Tensho, K., Nakaya, H., Nawata, M., Okabe, T., Wakitani, S., 2005. Low dose fibroblast growth factor-2 (FGF-2) enhances bone morphogenetic protein-2 (BMP-2)-induced ectopic bone formation in mice. Bone 36 (3), 399–407.
Nguyen, T.M., Arthur, A., Paton, S., Hemming, S., Panagopoulos, R., Codrington, J., Walkley, C.R., Zannettino, A.C., Gronthos, S., 2016. Loss of ephrinB1 in osteogenic progenitor cells impedes endochondral ossification and compromises bone strength integrity during skeletal development. Bone 93, 12–21.
Panagopoulos, V., Zinonos, I., Leach, D.A., Hay, S.J., Liapis, V., Zysk, A., Ingman, W.V., DeNichilo, M.O., Evdokiou, A., 2015. Uncovering a new role for peroxidase enzymes as drivers of angiogenesis. Int. J. Biochem. Cell Biol. 68, 128–138.
Panagopoulos, V., Liapis, V., Zinonos, I., Hay, S., Leach, D.A., Ingman, W., DeNichilo, M. O., Atkins, G.J., Findlay, D.M., Zannettino, A.C.W., Evdokiou, A., 2017a. Peroxidase enzymes inhibit osteoclast differentiation and bone resorption. Mol. Cell. Endocrinol. 440, 8–15.
Panagopoulos, V., Liapis, V., Zinonos, I., Hay, S., Leach, D.A., Ingman, W., DeNichilo, M. O., Atkins, G.J., Findlay, D.M., Zannettino, A.C., Evdokiou, A., 2017b. Peroxidase enzymes inhibit osteoclast differentiation and bone resorption. Mol. Cell. Endocrinol. 440, 8–15.
Patel, N., Brooks, R.A., Clarke, M.T., Lee, P.M., Rushton, N., Gibson, I.R., Best, S.M., Bonfield, W., 2005. In vivo assessment of hydroxyapatite and silicate-substituted hydroxyapatite granules using an ovine defect model. J Mater Sci Mater Med 16 (5), 429–440.
Prasad, G.C., Udupa, K.N., 1972. Studies on ultrastructural pattern of osteogenic cells during bone repair. Acta Orthop. Scand. 43 (3), 163.
Robubi, A., Berger, C., Schmid, M., Huber, K.R., Engel, A., Krugluger, W., 2014. Gene expression profiles induced by growth factors in in vitro cultured osteoblasts. Bone Joint Res 3 (7), 236–240.
Seeherman, H.J., Li, X.J., Bouxsein, M.L., Wozney, J.M., 2010. rhBMP-2 induces transient bone resorption followed by bone formation in a nonhuman primate core-defect model. J. Bone Joint Surg. Am. 92 (2), 411–426.
Shams-White, M.M., Chung, M., Fu, Z., Insogna, K.L., Karlsen, M.C., LeBoff, M.S., Shapses, S.A., Sackey, J., Shi, J., Wallace, T.C., Weaver, C.M., 2018. Animal versus plant protein and adult bone health: a systematic review and meta-analysis from the National Osteoporosis Foundation. PLoS One 13 (2), e0192459.
Simmons, C.A., Alsberg, E., Hsiong, S., Kim, W.J., Mooney, D.J., 2004. Dual growth factor delivery and controlled scaffold degradation enhance in vivo bone formation by transplanted bone marrow stromal cells. Bone 35 (2), 562–569.
Street, J., Bao, M., deGuzman, L., Bunting, S., Peale Jr., F.V., Ferrara, N., Steinmetz, H., Hoeffel, J., Cleland, J.L., Daugherty, A., van Bruggen, N., Redmond, H.P., Carano, R. A., Filvaroff, E.H., 2002. Vascular endothelial growth factor stimulates bone repair by promoting angiogenesis and bone turnover. Proc. Natl. Acad. Sci. U. S. A. 99 (15), 9656–9661.
Szpalski, C., Nguyen, P.D., Cretiu Vasiliu, C.E., Chesnoiu-Matei, I., Ricci, J.L., Clark, E., Smay, J.E., Warren, S.M., 2012. Bony engineering using time-release porous scaffolds to provide sustained growth factor delivery. J Craniofac Surg 23 (3), 638–644.
Takada, I., Kouzmenko, A.P., Kato, S., 2009. Wnt and PPARgamma signaling in osteoblastogenesis and adipogenesis. Nat. Rev. Rheumatol. 5 (8), 442–447.
Tannoury, C.A., An, H.S., 2014. Complications with the use of bone morphogenetic protein 2 (BMP-2) in spine surgery. Spine J. 14 (3), 552–559.
Theiss, F., Apelt, D., Brand, B., Kutter, A., Zlinszky, K., Bohner, M., Matter, S., Frei, C., Auer, J.A., von Rechenberg, B., 2005. Biocompatibility and resorption of a brushite calcium phosphate cement. Biomaterials 26 (21), 4383–4394.
Toth, J.M., Boden, S.D., Burkus, J.K., Badura, J.M., Peckham, S.M., McKay, W.F., 2009. Short-term osteoclastic activity induced by locally high concentrations of recombinant human bone morphogenetic protein-2 in a cancellous bone environment. Spine (Phila Pa 1976) 34 (6), 539–550.
Udagawa, N., Takahashi, N., Katagiri, T., Tamura, T., Wada, S., Findlay, D.M., Martin, T. J., Hirota, H., Taga, T., Kishimoto, T., Suda, T., 1995. Interleukin (IL)-6 induction of osteoclast differentiation depends on IL-6 receptors expressed on osteoblastic cells but not on osteoclast progenitors. J. Exp. Med. 182 (5), 1461–1468.
Wintges, K., Beil, F.T., Albers, J., Jeschke, A., Schweizer, M., Claass, B., Tiegs, G., Amling, M., Schinke, T., 2013. Impaired bone formation and increased osteoclastogenesis in mice lacking chemokine (C-C motif) ligand 5 (Ccl5). J. Bone Miner. Res. 28 (10), 2070–2080.
Wongwitwichot, P., Kaewsrichan, J., Chua, K.H., Ruszymah, B.H., 2010. Comparison of TCP and TCP/HA hybrid scaffolds for osteoconductive activity. Open Biomed Eng J 4, 279–285.
Yaszemski, M.J., Payne, R.G., Hayes, W.C., Langer, R., Mikos, A.G., 1996. Evolution of bone transplantation: molecular, cellular and tissue strategies to engineer human bone. Biomaterials 17 (2), 175–185.
Yu, X., Huang, Y., Collin-Osdoby, P., Osdoby, P., 2004. CCR1 chemokines promote the chemotactic recruitment, RANKL development, and motility of osteoclasts and are induced by inflammatory cytokines in osteoblasts. J. Bone Miner. Res. 19 (12), 2065–2077.
Yuan, H., Van Den Doel, M., Li, S., Van Blitterswijk, C.A., De Groot, K., De Bruijn, J.D., 2002. A comparison of the osteoinductive potential of two calcium phosphate ceramics implanted intramuscularly in goats. J Mater Sci Mater Med 13 (12), 1271–1275.
Zhang, X., Shu, X.O., Li, H., Yang, G., Li, Q., Gao, Y.T., Zheng, W., 2005. Prospective cohort study of soy food consumption and risk of bone fracture among postmenopausal women. Arch. Intern. Med. 165 (16), 1890–1895.
Zhu, W., Boachie-Adjei, O., Rawlins, B.A., Frenkel, B., Boskey, A.L., Ivashkiv, L.B., Blobel, C.P., 2007. A novel regulatory role for stromal-derived factor-1 signaling in bone morphogenic protein-2 osteogenic differentiation of mesenchymal C2C12 cells. J. Biol. Chem. 282 (26), 18676–18685.
Zhu, W., Liang, G., Huang, Z., Doty, S.B., Boskey, A.L., 2011. Conditional inactivation of the CXCR4 receptor in osteoprecursors reduces postnatal bone formation due to impaired osteoblast development. J. Biol. Chem. 286 (30), 26794–26805.